# MiR-362-5p targets CDK2 and inhibits tumorigenesis in renal cell carcinoma

**Yang Liu**
Heilongjiang Red Cross Sengong General Hospital
**Ja Tang**
Heilongjiang Red Cross Sengong General Hospital
**Dandan Yang** ( 1121562820@qq.com )
Heilongjiang Red Cross Sengong General Hospital

**Research Article**

**Keywords:**

**Posted Date:** February 15th, 2022

**DOI:** https://doi.org/10.21203/rs.3.rs-1237942/v1

# Abstract

**Background:** Renal cell carcinoma (RCC) is a very common malignant tumor. Identifying novel biomarkers is essential to predict the progression and prognosis of RCC. MicroRNA (miRNA) expression profiles have been extensively studied in major cancers. The purpose of this study was to evaluate the expression of miR-362-5p in clear cell renal cell carcinoma (ccRCC) and to evaluate its potential mechanisms in RCC.

**Material and Methods:**

In this study, 4 groups of clear ccRCC and adjacent miRNA expression profiling chips were screened using the GEO database. Six miRNAs in 4 sets of expression spectrum chips were expressed at low levels in ccRCC tissues, among which miR-362-5p exhibited the greatest downregulation. The effects of miR-362-5p were observed by real-time fluorescence quantitative PCR, cell transfection experiments, CCK-8 experiments and flow cytometry cell cycle assays. Target genes of miR-362-5p were verified by luciferase reporter assay and confirmed by western blot.

**Results:**

Through data analysis, miR-362-5p was selected for study. Cell growth curves and flow cytometry detection showed that overexpression of miR-362-5p inhibited the growth of RCC cells and induced cell cycle arrest at the G0/G1 phase. Bioinformatics analysis indicated that cyclin-dependent kinase 2 (CDK2) could be a potential target of miR-362-5p. Mechanistic studies revealed that miR-362-5p is directly responsible for inhibiting CDK2 expression in ccRCC cell lines.

**Conclusion:**

In summary, our study confirmed that miR-362-5p in ccRCC tissues is significantly downregulated. MiR-362-5p regulates CDK2 to inhibit the proliferation of clear cell renal cell carcinoma. CDK2 regulates tumor cell growth and cell cycle progression, which arrests the cell cycle at the G1/S phase.


# Introduction

Renal cell carcinoma (RCC) is a common malignant tumor of the genitourinary system. The incidence of RCC has increased at an annual rate of 2-4% in the past 20 years(1). Renal cell carcinoma has become the third most common urinary system malignancy after prostate cancer and bladder cancer, accounting for approximately 3% of adult malignancies. Clear cell renal cell carcinoma (ccRCC) is the most common histological subtype of renal cell carcinoma, accounting for 75-80% of renal cell carcinomas(2). Due to the lack of diagnostic biological markers and specific symptoms at the beginning of the disease, approximately 20%-30% of RCC patients have already experienced metastasis upon diagnosis(3). In addition, renal cell carcinoma is not sensitive to conventional radiotherapy or chemotherapy, and surgery remains the most effective treatment for these patients(4, 5). Unfortunately, 20%-40% of RCC patients will

relapse and metastasize after surgery(6). Therefore, exploring the mechanism of RCC occurrence and development and formulating more effective treatment strategies are urgently needed.

MicroRNAs (miRNAs) are evolutionarily conserved, noncoding, small RNAs with a length of 20-22 nucleotides(7). They target particular messenger RNAs (mRNAs) and degrade RNA or inhibit translation, regulating gene expression after transcription (8). Increasing data demonstrate that miRNAs play key roles in both physiological and pathological processes, and the dysregulation of miRNAs is involved in many diseases, including cancer(9). Recent evidence shows that early cancer detection is one of the uses of miRNAs, which serve as biomarkers to accurately estimate prognosis and cancer treatment targets. In addition, studies have shown that miRNAs can act as oncogenes or tumor suppressor genes during tumor occurrence and development(10). Recently, increasing evidence has shown that miRNAs are dysregulated in clear cell carcinoma of the kidney, and the survival rates of RCC sufferers are associated with the levels of miRNA expression. For instance, high miR21/10B expression is associated with poor prognosis(11). MiR-30a-5p is expressed in a variety of tissues, and its expression in ccRCC is significantly reduced. It suppresses the proliferation of ccRCC and induces apoptosis by downregulating the expression of GRP78(12). However, to date, the expression and mechanism of miR-362-5p in clear cell carcinoma of the kidney are still not known.

In this study, we screened 4 groups of renal clear cell carcinoma and miRNA expression profiling chips from the GEO database. After data analysis, we found that 6 miRNAs in the 4 sets of expression profile chips all exhibited low expression in ccRCC tissues, of which miR-362-5p was the most downregulated. We subsequently focused on miR-362-5p as a delegate to research its role 5p in cell proliferation, the cell cycle and oncogenesis and evaluated its potential mechanism in renal cell carcinoma. We found that miR-362-5p is a key inhibitor of cell growth in vitro and in vivo in RCC. Of note, we investigated the antitumor function of miR-362-5p for the first time using cyclin-dependent kinase 2(CDK2), a key checkpoint regulator of G1/S cell cycle progression.

# Materials And Methods

### Clinical specimens

We collected noncancerous tissue next to cancer samples of clear cell carcinoma kidney tissues from patients whose pathological diagnosis was ccRCC and who had undergone radical nephrectomy treatment. Tissue samples were rapidly frozen in liquid nitrogen and then stored in a deep freezer at −80°C. All specimens were examined by professional pathologists and graded according to AJCC and Fuhrman classification. This study was approved by the Heilongjiang Red Cross Sengong General Hospital institutional ethics review committee, and written informed consent was obtained from all patients.

### Accessing and investigating an online cancer database

We downloaded RNA-seq data for 249 tumors and 71 matched noncancerous specimens from the TCGA Data Portal website (https://tcga-data.nci.nih.gov/tcga/). We quantified miRNA expression data through quality control, comparison and expression quantification. Meanwhile, we downloaded four groups from the GEO database (https://www.ncbi.nlm.nih.gov/geo/) miRNA expression spectrum datasets: GSE71302, GSE23085, GSE16441, and GSE47582. Among the 4 groups of miRNAs expressed, we screened out miRNA expression profiles in ccRCC whose microarray expression was significantly reduced.

## Western blotting

We used 10% SDS–PAGE to dilute the corresponding proportion of protein lysates (1:4) for electrophoresis and transferred the proteins to PVDF membranes (Millipore, MA) with cold transfer buffer. The membrane was sealed with 5% skim milk in TBS-T for 1 hour at room temperature (RT) and then incubated with the relevant primary antibodies overnight at 4°C. After washing the membranes, we subsequently incubated them with secondary antibodies bound to horseradish peroxidase (HRP). Enhanced chemiluminescence was used to visualize the proteins. Western blotting was performed using the following antibodies: anti-actin (Sigma–Aldrich, 1:8,000) and anti-CDK2 (Bioworld, MN). We subsequently used goat anti-mouse IgG (HRP) and goat anti-rabbit IgG (HRP) diluted at 1:2000 as secondary antibodies.

RNA isolation and quantitative real-time PCR

We used TRIzol Reagent (Invitrogen, CA, USA) to extract total RNA from fresh specimens frozen in liquid nitrogen. Next, we reverse transcribed the total RNA (1 μg) into cDNA using a high power capacity cDNA Reverse Transcriptase Kit (TOYOBO, JAPAN). Quantitative RT–PCR (qRT–PCR) was performed using SYBR Green PCR Master Mix (Invitrogen) on a Roche LightCycler 480 system (Roche Diagnostics, Germany) to determine the comparative standard of miR-362-5P normalized to the U6 gene. Each sample was tested three times. Endogenous controls were U6 snRNA or GAPDH (Table I). All samples were normalized to internal controls, and fold changes were calculated by relative quantification.

Cell culture techniques and transfection

A variety of human renal cell carcinoma cell lines, including OS-RC-2 and 786-O, were cultured with RPMI 1640 (Gibco, Carlsbad, California) in a humidified atmosphere with 10% fetal bovine serum (FBS), 37℃, and 5% $CO_2$. GenePharma Biotech (Shanghai, China) synthesized four synthetic short single-stranded RNA oligonucleotides or double-stranded RNA oligonucleotides with chemical modification (miR-362-5p mimics, mimics NC, miR-362-5p inhibitor, inhibitor NC) (Table II). We plated $2x10^5$ cells/well into 6-well plates and then transfected them with 160 nmol/L miRNAs using Lipofectamine™ 2000 (Invitrogen). The CDK2 overexpression vector was constructed by inserting the PCR-amplified coding sequence CDK2 into the pcDNA3.1 vector.

## Immunohistochemistry

Paraffin embedding of 45 ccRCC and 15 noncancerous renal tissues was performed and cut at a section thickness of 4 mm to analyze the expression of CDK2 (Bioworld, 1:100 dilution) . We used a digital camera DXM1200 system (Nikon) to evaluate CDK2 expression under a light microscope. For human specimens, a modified histological score (H-score) was used to score the IHC results. The IHC score includes a semiquantitative assessment of the proportion of positive cells and staining intensity. Under the same staining conditions, the three grades were assigned as negative/weak, medium, or strong(13).

## CCK-8

The 96-well plates were inoculated with $8\times10^3$ cells per well, with a volume of 100 μl. Ten microliters of CCK-8 (Dojindo Molecular Technologies, Inc., Kyushu, Japan) was added to each well and incubated for 2 hours at 37℃ the next day. A multimode reader (Bio-Tek, USA) was used to determine the effects of miR-362-5p on cell growth and viability at 450 nm(14).

## Cell cycle assay

In the cell cycle assay, cells were cultured in 6-well plates at $2\times10^5$ cells per well. When cell confluence reached about 80%, cells were collected using trypsin, washed with cold PBS 3 times, and fixed overnight at -20℃ in 70% ethanol. PBS was used to rehydrate the fixed cells, which were stained with PI/RNase, and analyzed by flow cytometry (Becton Dickinson, Mountain View, CA, USA). The experiment was independently repeated 3 times.

## Luciferase assay

We synthesized two types of CDK2-3 UTRs: wild-type CDK2-3 UTR (WT) and mutant CDK2-3 UTR (MUT) containing miR-362-5p. Then, we cloned them downstream of the firefly luciferase gene into the pGL3 promoter vector (Ambion). We used two RCC cell lines, 786 cells and OS-RC-2 cells, which were plated in 48-well plates and grown to 80% confluence. Then, the cells were cotransfected with luciferase plasmid and miR-362-5p or control miRNA. Luciferase activity in two types of CDK2-3 UTR firefly luciferases was determined by double luciferase assay (Promega) 48 h after transfection.

## Xenotransplantation of tumor cells

The genomic sequences encoding miRNA-362-5p and negative control NC were amplified and cloned into a lentivirus vector (GenePharma Biotech; Shanghai, China). Gene sequencing confirmed that the lentivirus successfully infected OS-RC-2 cells. All experimental procedures involving animals were approved by the Animal Care and Use Committee of Heilongjiang Red Cross Sengong General Hospital. Four- to five-week-old female nude mice (20, aged 6 weeks) were purchased from Beijing HFK Biotechnology Co. Ltd. (Beijing). OS-RC-2 cell suspension (stably transfected with miR-362-5p or negative control (NC)) was subcutaneously injected ($5\times10^6$ cells in 200 μL total volume). Xenograft tumor growth in mice was assessed every day. After one week, the tumor diameter was measured every 3 days using calipers, and the tumor volume was calculated as length×width$^2$×0.5. Twenty-eight days after after injection, the mice

were euthanized using anesthesia, and the tumors were removed and weighed. Relative expression levels of miR-362-5p were assessed by qRT–PCR, and the volume and weight of the recorded tumors were collated and plotted.

### Statistical analysis

The chi-square test was used to determine the clinical and pathological association between miR-362-5p and CDK2. Survival differences are shown by the Kaplan–Meier method and were analyzed using the log-rank test. The total survival time was calculated as the time from surgery to death. In the *in vitro and in vivo* experiments, we used Student's t test to analyze differences between groups. The Spearman correlation coefficient was calculated for correlation analysis. Data are expressed as the mean ± SEM, and all results were confirmed by at least three independent experiments. The SPSS 18.0 software system (SPSS, Chicago, IL) was used for statistical analysis. $p< 0.05$ was considered statistically significant (Table III).

# Results

### Screening differentially expressed miRNAs in renal clear cell carcinoma.

To explore the expression of miRNAs in ccRCC, we first selected 4 samples of ccRCC and 4 matched noncancerous samples from GEO (https://www.ncbi.nlm.nih.gov/geo/) to analyze the expression of the miRNA profile dataset, which included GSE71302, GSE23085, GSE16441, and GSE47582. A fold change between tumor and adjacent noncancerous tissues greater than 2 and $P<0.05$ were used as the criteria for screening differentially expressed miRNAs. We focused on miRNAs that were significantly downregulated in tumor tissues. We took the intersection of miRNAs whose expression was downregulated in ccRCC from the 4 miRNA expression profiling chips, and the 6 miRNAs showed statistically significant downregulation in the data of the 4 miRNA expression profiling chips of renal clear cell carcinoma, of which miR-362-5p was one of the most downregulated miRNAs (Figure 1A). The details of the 6 miRNAs were listed in Table IV.

### MiR-362-5p is downregulated in ccRCC and is related to patient survival and prognosis.

To further verify the microarray data, we downloaded sequencing data for 249 cases of renal clear cell carcinoma and 71 cases of noncancerous renal tissues from the TCGA data and assessed the levels of miR-362-5p. Our results showed that levels of miR-362-5p were significantly lower in tumor tissues than in adjacent noncancerous kidney tissue.(Figure 1B). We also used qRT–PCR to determine the expression levels of miR-362-5p in 50 pairs of renal clear cell carcinoma and paracarcinoma paired samples. Consistent with the TCGA and microarray data, the average expression levels of miR-362-5p were significantly lower than that in adjacent tissues (Figure 1C; $p<0.05$). To show the correlation in the expression of miR-362-5p as well as clinicopathological characteristics, we examined the sex, age, TNM stages, Fuhrman grade, lymph node metastasis and distant metastasis for the corresponding miR-362-5p expression tissues in ccRCC, which is summarized in Table III. As shown in the table, low expression of

miR-362-5p was related to high TNM stage ($P = 0.045$) and pathological level ($P = 0.032$) progression in ccRCC patients (Table III). This means that miR-362-5p may be primarily involved in the growth of ccRCC, especially when the tumor is at an early stage. Clinically, the survival and prognosis of patients with renal clear cell carcinoma is worthy of attention. To determine the correlation between the expression of miR-362-5p and patient survival and prognosis, we divided 50 renal cell carcinoma patients into high expression and a low expression groups according to the expression value of miR-362-5p. Kaplan–Meier survival analysis confirmed that patients with low miR-362-5p expression had a shorter overall survival time than patients with high miR-362-5p expression (Figure 1D).

## MiR-362-5p inhibits cell proliferation by interrupting cell cycle progression in renal clear cell carcinoma cells.

Some reported miRNA analysis of clear cell renal cell carcinoma have shown that in ccRCC, miR-362-5p is one of the downregulated miRNAs (15), in agreement with our data. However, the characterization of miR-362-5p in renal clear cell carcinogenesis and its mechanism have not been fully resolved. To determine the biological function of miR-362-5p in vitro, we first assessed its expression by qRT–PCR in 5 widely used renal clear cell carcinoma cell lines. The results showed that expression of miR-362-5p in the 786-O, OS-RC-2, and OS-RC-1 cell lines was significantly reduced compared to the average expression in the noncancerous kidney cell line HK2 (Figure 2A). Next, to examine the characteristics of miR-362-5p in ccRCC, we performed functional gain and functional loss experiments by transfecting agomiR-362-5p and antagomiR-362-5p. 786-O and OS-RC-2 cells were transfected with inhibitors targeting miR-362-5p (miR-362-5p depressant, miR-362-5p-i) or negative controls (miR-362-5p NC, NC-i). Quantitative analysis of the transcription levels of miR-362-5p by qRT–PCR confirmed the efficacy of miR-362-5p-i knockout (Figure 2B). As shown in Figure 2B, in 786-O and OS-RC-2 cells, miR-362-5p expression declined by at least 60%. Similarly, miR-362-5p mimics (miR-362-5p mimic, miR-362-5p) or negative control (miR-362-5p NC, NC) were transfected into 786-O and OS-RC-2 cells. Quantitative analysis of the transcription levels of miR-362-5p by qRT–PCR confirmed the efficacy of miR-362-5p overexpression. As shown in Figure 2C, the levels of miR-362-5p in 786-O and OS-RC-2 cells were increased at least 300-fold. MiR-362-5p reduced the growth of 786-O and OS-RC-2 cells at 72 h by 22.4% ($p < 0.01$) and 19.7% ($p < 0.01$), respectively, as confirmed by CCK-8 cell proliferation results (Figure 2D), indicating that miR-362-5p restrains the proliferation of RCC cells. We next performed a supplemental functional analysis loss experiment. After knocking down miR-362-5pi, CCK-8 detection of cell proliferation results revealed that miR-362-5p increased proliferation in OS-RC-2 and 786-O cells at 72 h by 18.6% ($p < 0.01$) and 16.4% ($p < 0.01$), respectively (Figure 2D). In contrast, miR-362-5p did not significantly affect cell growth compared to the blank control NC. To further determine the mechanism by which miR-362-5p induces and inhibits cell growth, flow cytometry was used to analyze the influence of miR-362-5p on the cell cycle progression of 786-O and OS-RC-2 cells. In contrast to the control group, after overexpression of miR-362-5p in 786-O cells, the G0/G1 phase was significantly increased from 56–67.73% ($p < 0.01$), and in OS-RC-2 cells from 58.74–67.4% ($p < 0.01$). S-phase cells were significantly reduced in 786-O cells, decreasing from 38.02–28.73% ($p < 0.01$), and OS-RC-2 cells exhibited S phase decreases from 35.28–27.67% ($p < 0.05$). In contrast, the rate of cells in the G2/M stage did not change significantly in either cell line (Figure 2E). In

addition, to confirm the characterization of miR-362-5p during the cell cycle, we used antagomiR-362-5p to block miR-362-5p. The results showed that inhibiting the expression of miR-362-5p ca rescued 786-O and OS-RC-2 cell cycle arrest. In summary, these data show that overexpression of miR-362-5p stalls the RCC cell cycle in G1/S phase, which produces antitumor proliferation effects.

**MiR-362-5p restrains tumor growth in a xenograft mouse model.**

Our previous in vitro studies revealed that miR-362-5p may play a tumor suppressive role in renal clear cell carcinoma cells. Next, we investigated whether miR-362-5p inhibits the growth of renal clear cell carcinoma xenograft tumors in nude mice. We constructed a stably transfected renal cell carcinoma OS-RC-2 cell line (stably transfected with miR-362-5p or negative control NC) and injected the transfected cells into nude mice to observe the growth of the transplanted tumors. Mice were sacrificed 28 days after injection, and the tumors were collected and analyzed (Figure 3A). After the experiment, mice were dissected, tumor weight was measured, and RNA was immediately extracted from the tumor tissue. qRT–PCR results confirmed that expression of miR-362-5p in the stably transfected xenograft tumor tissues was significantly higher than that in the control xenograft tissues ($P < 0.01$) (Figure 3B). As shown in Figure 3, the tumor size of the miR-362-5p stable cells injected into mice was significantly smaller than that of the NC stable cells in the control group. The tumor volume and weight of the xenografts transfected with miR-362-5p were significantly lower than those of the negative control group ($P<0.01$) (Figure 3C, D).

**CDK2 is a direct targeting gene of miR-362-5p's in RCC cells** As key factors for posttranscriptional regulation of genes, miRNAs perform various necessary functions. We used starBase v2.0 (http://starbase.sysu.edu.cn/) to identify the latent primary targets of miR-362-5p and to determine the latent mechanism by which miR-362-5p inhibits renal transparent cell carcinoma. The 3'UTR structure of CDK2 was found to possess a potential binding site with miR-362-5p and had a high reliability score, so we selected this gene as a target. CDK2 is essential for DNA replication during the G1/S cell cycle transition (Figure 4A). CDK2 was confirmed to be an immediate target gene for miR-362-5p. Our research cloned wild-type or mutant 3'UTR of CDK2 into the 3'end of the LUC gene and constructed two luciferase reporter plasmids (Figure 4A). In both 786-O and OS-RC-2 cells, miR-362-5p showed that luciferase activity in wild-type (WT) cells was lowered but was not reduced in the Mut 3'-UTR of CDK2 (Figure 4B).

To test and verify the decreased expression of CDK2 in response to miR-362-5p in ccRCC, using the TCGA database, expression of miR-362-5p and CDK2 was compared, and we observed that the transcript accumulation of CDK2 was negatively correlated with the levels of miR-362-5p in clear cell carcinoma of the kidney ($r = -0.245$, $P < 0.0001$, Figure 4C). Subsequently, CDK2 expression in clear cell carcinoma of the kidney and adjacent tissues of human ccRCC patients was analyzed using immunohistochemistry, and the levels of CDK2 protein in adjacent tissues were lower than those in ccRCC tissues (Figure 4D). Next, we explored the regulation of CDK2 in miR-362-5p in ccRCC cells. Overexpression of miR-362-5p reduced the protein levels of CDK2 in ccRCC cells. In contrast, in 786-O and OS-RC-2 cells, using antimiR-362-5p to inhibit the levels of miR-362-5p led to an increase in the levels of CDK2 protein (Figure 4E).

**The anti-ccRCC function of miR-362-5p is mediated by inhibiting CDK2 expression.**

We demonstrated that CDK2 is an immediate target gene of miR-362-5p; in addition, not only miR-362-5p overexpression but also CDK2 knockout inhibited clear cell carcinoma of the kidney (Figure 4A-E). Next, we investigated whether the antitumor function of miR-362-5p is mediated by regulating the levels of CDK2 in clear cell carcinoma of the kidney. First, we transduced a negative control or miR-362-5p and overexpressed the CDK2 plasmid. Our results showed that overexpression of miR-362-5p induced decreased CDK2 mRNA and protein expression levels, while cotransfection of CDK2 overexpression plasmid and miR-362-5p plasmid significantly rescued the decreased CDK2 expression. In addition, its effects were lower than those of the negative control (Figure 5A and B). This shows that miR-362-5p effectively decreases the levels of CDK2. After cotransfection with the CDK2 plasmid, the inhibitory effect of overexpressing miR-362-5p on the proliferation of ccRCC 786-O cells and OS-RC-2 cells was eliminated (Figure 5C). At the same time, cotransfection of the CDK2 plasmid eliminated cell cycle suppression caused by miR-362-5p (Figure 5D). This indicates that reducing the expression of CDK2 mediates the inhibitory influence of miR-362-5p on ccRCC.

# Discussion

In ccRCC, miRNAs can inhibit the expression levels of target genes through degradation or translation inhibition, making them important tumor regulators that have attracted extensive attention(16). In this study, we screened 4 groups of ccRCC and adjacent tissues using miRNA expression profile chips from the GEO database. After data analysis, it was found that 6 miRNAs exhibited low expression in the 4 groups of ccRCC tissues. The downregulation of miR-362-5p was the most significant (Figure 1A). Moreover, it was verified that miR-362-5p is significantly downregulated in both ccRCC tissues and renal cancer cell lines. MiR-362-5p was also closely related to the clinical TNM grading and pathological stage of patients, and the miR-362-5p expression levels were negatively correlated with ccRCC prognosis of (Figure 1D). MiR-362-5p inhibits the growth of ccRCC cells by regulating the expression of the ccRCC direct target gene CDK2. Here, we demonstrated that miR-362-5p directly targets CDK2 to inhibit cell growth and tumorigenesis in vitro. Our results indicate that miR-362-5p may be a tumor suppressor in ccRCC.

MiRNAs are essential regulators of protein expression and are closely related to abnormal tumor regulation and tumorigenesis(17). MiR-362-5p has been confirmed to play a vital role in the proliferation, metastasis and survival of patients with acute myeloid leukemia, breast cancer, liver cancer and other cancers. Fang et al. showed that miR-362-5p promotes the proliferation, migration and invasion of breast cancer cells; thus, miR-362-5p may represent a new potential therapeutic target for the treatment of breast cancer(18). Ma et. al. reported that high expression of miR-362-5p in patients who suffer from acute myeloid leukemia (AML) is correlated with a poor overall survival rate. These results suggest that miR-362-5p is a carcinogenic factor for AML development(19). Meanwhile, studies in non-small cell lung carcinoma (NSCLC) have found that expression of miR-362-5p in NSCLC is higher than that in adjacent tissues(20). Further analysis revealed that miR-362-5p affects the invasion, migration and colony

formation of NSCLC cells and promotes tumor formation by regulating the expression of Sema3A in NSCLC cells(20). Some scholars have found that expression of miR-362-5p is downregulated in cisplatin-resistant gastric cancer cell lines, while upregulation of miR-362-5p significantly increased the chemotherapeutic sensitivity to cisplatin and apoptosis induced by cisplatin(21). We also found that the same miRNA has different roles in different tumors, depending on the key factors driving tumorigenesis in a specific cellular environment. In this study, we confirmed that expression of miR-362-5p is inhibited in ccRCC tissues and renal cancer cell lines. At the same time, miR-362-5p suppressed tumors in ccRCC. Although some previous studies have demonstrated that miR-362-5p is one of the miRNAs with the lowest expression in ccRCC, the role of miR-362-5p in ccRCC and its specific mechanism are still unclear.

Cell cycle dysregulation affects cell growth and tumorigenesis(22, 23). Our results showed that miR-362-5p inhibits cell growth because miR-362-5p causes G0/G1 cycle arrest in RCC cells, blocking entry into S phase. It was suggested that downregulation of miR-362-5p promotes the proliferation of RCC cells, which was related to G1/S checkpoint dysfunction. As a serine/threonine protein kinase family, cyclin-dependent kinase 2 (CDK2) is activated at specific points in the cell cycle. Due to its function as a catalytic subunit of the cyclin-dependent protein kinase complex, CDK2 is essential for the G1/S phase transition of the cell cycle. However, its activity is restricted to the G1/S phase. CDK2 plays a redundant role in cell division and mouse development(24, 25). Consistent with other studies, we found that CDK2 expression was upregulated in ccRCC by immunohistochemical analysis. Moreover, in the TCGA data, the correlation between the analysis of miR-362-5p and CDK2 expression in ccRCC showed that miR-362-5p was negatively correlated with CDK2 expression (r=-0.245). We used multiple independent analyses to confirm that miR-362-5p is a specifically negative regulator of CDK2 both in vivo and in vitro, while miR-362-5p and CDK2 antagonize each other and can reverse each other's effects. In summary, downregulation of miR-362-5p, which directly targets CDK2 genes in RCC, may lead to increased tumor volume.

According to our study, the 3'-UTR of CDK2 is the direct target of miR-362-5p. miR-362-5p plays a role in directly inhibiting the expression of CDK2 in ccRCC cells, inhibiting the growth of ccRCC cells and tumors. Therefore, the interaction between miR-362-5p and CDK2 may represent a new therapeutic target for ccRCC.

# Conclusion

In summary, we found that miR-362-5p targets CDK2 in clear cell renal cell carcinoma, inhibiting tumor cell growth by directly inhibiting the expression of CDK2 and exerting an antitumor effect. MiR-362-5p downregulates CDK2; therefore, miR-362-5p eliminates the malignant biological behavior changes caused by increased CDK2 expression in ccRCC. In conclusion, our results suggest the potential value of miR-362-5p in the treatment of ccRCC. In RCC with abnormal expression of miR-362-5p, DNA replication is inhibited by blocking the expression of CDK2, which inhibits tumor growth, representing an alternative strategy for the treatment of clear cell renal cell carcinoma.

# Declarations

### Ethics approval and consent to participate

This study was approved by the Ethics Committee of Heilongjiang Red Cross Sengong General Hospital and the methods were carried out in accordance with the approved guidelines. All the patients have been informed and signed informed consent before the experiments.The animal experimental processes were approved by the Ethnic Committee of Heilongjiang Red Cross Sengong General Hospital and conducted in strict accordance to the standard of the Guide for the Care and Use of Laboratory Animals published by the Ministry of Science and Technology of the People's Republic of China in 2006.Meanwhlie, the study is reported in accordance with ARRIVE guidelines (https://arriveguidelines.org).

### Consent for publication

Not applicable.

### Availability of data and materials

The datasets generated/analysed during the current study are available. The GEO database (https://www.ncbi.nlm.nih.gov/geo/) miRNA expression spectrum datasets: GSE71302, GSE23085, GSE16441, and GSE47582. The details of the 6 miRNAs were listed in Table IV.

### Competing interests

The authors declare that they have no competing interests.


### Funding

There was no funding for the study.


### Authors' contributions

YL and JT designed the research studies and analyzed and interpreted the data. YL and DY conducted experiments and acquired the data. YL drafted the manuscript, and all authors contributed to revisions.


### Acknowledgments

Not applicable.


# References


1. Bhatt JR, Finelli A. Landmarks in the diagnosis and treatment of renal cell carcinoma. Nature Reviews Urology. 2014;11(9):517.
2. Audenet F, Yates DR, Cancel-Tassin G, Cussenot O, Rouprêt M. Genetic pathways involved in carcinogenesis of clear cell renal cell carcinoma: genomics towards personalized medicine. Bju

International. 2012.

3. Zheng T, Yang CG, Biology LOC, Research SKLoD, Medica SIOM, Sciences CAO, et al. Targeting SPOP with small molecules provides a novel strategy for kidney cancer therapy. Science China(Life Sciences). 2017.
4. De Meerleer G, Khoo V, Escudier B, Joniau S, Bossi A, Ost P, et al. Radiotherapy for renal-cell carcinoma. Lancet Oncology. 2014;15(4):e170-e7.
5. Buti S, Bersanelli M, Sikokis A, Maines F, Facchinetti F, Bria E, et al. Chemotherapy in metastatic renal cell carcinoma today? A systematic review. Anti-cancer Drugs. 2013;24(6):535–54.
6. Jin L, Xu X, Ye B, Pan M, Shi Z, Hu Y. Elevated serum interleukin-35 levels correlate with poor prognosis in patients with clear cell renal cell carcinoma. International Journal of Clinical & Experimental Medicine. 2015;8(10):18861.
7. Bartel DP. MicroRNAs: Genomics, Biogenesis, Mechanism, and Function. Cell. 2004.
8. Ying SY, Chang DC, Lin SL. The microRNA (miRNA): overview of the RNA genes that modulate gene function. Molecular Biotechnology. 2008;38(3):257.
9. Aguda BD. Modeling microRNA-transcription factor networks in cancer. Oxygen Transport to Tissue XXXIII. 2013;774(774):149–67.
10. Jing Q, Lu J, Xiang P, Tao H, Lai Y, Chen P, et al. Oncogenic miR-23a-5p is associated with cellular function in RCC. Molecular Medicine Reports. 2017;16(2):2309–17.
11. Fritz H, Lindgren D, Ljungberg B, Axelson H, Dahlbäck B. 595: The miR21/10b ratio as a prognostic marker in metastasis-free clear cell renal cell carcinoma patients. European Journal of Cancer. 2014.
12. Wang C, Cai L, Liu J, Wang G, Li H, Wang X, et al. MicroRNA-30a-5p Inhibits the Growth of Renal Cell Carcinoma by Modulating GRP78 Expression. Cellular Physiology & Biochemistry. 2017;43(6):2405–19.
13. Wang C, Cai L, Liu J, Wang G, Li H, Wang X, et al. MicroRNA-30a-5p Inhibits the Growth of Renal Cell Carcinoma by Modulating GRP78 Expression. Cellular physiology and biochemistry: international journal of experimental cellular physiology, biochemistry, and pharmacology. 2017;43(6):2405–19. doi: 10.1159/000484394. PubMed PMID: 29073630.
14. Zhao L, Zhang Y, Zhang Y. Long noncoding RNA CASC2 regulates hepatocellular carcinoma cell oncogenesis through miR-362-5p/Nf-kappaB axis. J Cell Physiol. 2018;233(10):6661–70. doi: 10.1002/jcp.26446. PubMed PMID: 29319182.
15. Guanghui, Ying, Ruilan, Wu, Min, Xia, et al. Identification of eight key miRNAs associated with renal cell carcinoma: A meta-analysis. Oncology Letters. 2018.
16. Xue D, Wang H, Chen Y, Shen D, Lu J, Wang M, et al. Circ-AKT3 inhibits clear cell renal cell carcinoma metastasis via altering miR-296-3p/E-cadherin signals. Mol Cancer. 2019;18(1):151. doi: 10.1186/s12943-019-1072-5. PubMed PMID: 31672157; PubMed Central PMCID: PMC6824104.
17. Acunzo M, Romano G, Wernicke D, Croce CM. MicroRNA and cancer–a brief overview. Advances in biological regulation. 2015;57:1–9. doi: 10.1016/j.jbior.2014.09.013. PubMed PMID: 25294678.

18. Ni F, Gui Z, Guo Q, Hu Z, Wang X, Chen D, et al. Downregulation of miR-362-5p inhibits proliferation, migration and invasion of human breast cancer MCF7 cells. Oncology Letters. 2016;11(2):1155–60. doi: 10.3892/ol.2015.3993.
19. Ma Q-L, Wang J-H, Yang M, Wang H-p, Jin J. MiR-362-5p as a novel prognostic predictor of cytogenetically normal acute myeloid leukemia. Journal of Translational Medicine. 2018;16(1). doi: 10.1186/s12967-018-1445-3.
20. Luo D, Zhang Z, Zhang Z, Li J-Y, Cui J, Shi W-P, et al. Aberrant Expression of miR-362 Promotes Lung Cancer Metastasis through Downregulation of Sema3A. Journal of Immunology Research. 2018;2018:1–10. doi: 10.1155/2018/1687097.
21. Wei X, Gao M, Ahmed Y, Gao M, Liu W, Zhang Y, et al. MicroRNA3625p enhances the cisplatin sensitivity of gastric cancer cells by targeting suppressor of zeste 12 protein. Oncology Letters. 2019. doi: 10.3892/ol.2019.10496.
22. Douglas, Hanahan, and, Robert, Weinberg. The Hallmarks of Cancer. Cell. 2000.
23. Carleton M, Cleary MA, Linsley PS. MicroRNAs and cell cycle regulation. Cell Cycle. 2007;6(17):2127–32.
24. Campaner S, Doni M, Hydbring P, Verrecchia A, Bianchi L, Sardella D, et al. Cdk2 suppresses cellular senescence induced by the c-myc oncogene. Nature Cell Biology. 2010;12(1):1–14.
25. Ortega S, Prieto I, Odajima J, Martín A, Barbacid M. Cyclin-dependent kinase 2 is essential for meiosis but not for mitotic cell division in mice. Nature Genetics. 2003;35(1):25–31.

# Tables

**Table I Sequences of primers used in the present study**

| Small RNA | Sequence(5'-3') |
|---|---|
| miR-362-5p-qPCR-F | UCUCAGCUGUAAACAUCCUACAC |
| Uni-miR-qPCR-R | GCGAGCACAGAATTAATACGACTCAC |
| CDK2-qPCR-F | CCAGGAGTTACTTCTATGCCTGA |
| CDK2-qPCR-R | TTCATCCAGGGGAGGTACAAC |
| GAPDH-qPCR-F | CCCAGCCTCAAGATCATCAGCAATG |
| GAPDH-qPCR-R | ATGGACTGT GGTCATGAGTCCTT |

**Table II Sequences of miRNA mimics, inhibitors**

| Small RNA | Sequence(5'-3') |
|---|---|
| miR-362-5p NC | UUCUCCGAACGUGUCACGUTT |
| miR-362-5p mimic | CUUCCAGUCGAGGAUGUUUACA |
| miR-362-5p NC-i | ACGUGACACGUUCGGAGAATT |
| miR-362-5p inhibitor | AGAGCUUCGACCUUCCUAAGTT |

**Table III. Correlation between clinicopathological characteristics and miR-362-5p expression levels in ccRCC patients.**

| Characteristics | Number of patients | miR-362-5p | | χ2 | P-value |
|---|---|---|---|---|---|
| | | High expression(%) | Low expression(%) | | |
| **Gender** | | | | 0.053 | 0.817 |
| Male | 30 | 14(58.33) | 16(61.54) | | |
| Female | 20 | 10(41.67) | 10(38.46) | | |
| **Age** | | | | 0.001 | 0.982 |
| ≤ 65 | 27 | 14(53.85) | 13(54.17) | | |
| >65 | 23 | 12(46.15) | 11(45.83) | | |
| **TNM Stage** | | | | 4.023 | 0.045 |
| □+□ | 29 | 18(72.00) | 11(44.00) | | |
| □+□ | 21 | 7(28.00) | 14(56.00) | | |
| **Grade** | | | | 4.591 | 0.032 |
| Grade1+2 | 35 | 22(84.62) | 15(57.69) | | |
| Grade3+4 | 15 | 4(15.38) | 11(42.31) | | |
| **Lymph node metastasis** | | | | 0.772 | 0.38 |
| No | 46 | 24(88.89) | 22(95.65) | | |
| Yes | 4 | 3(11.12) | 1(4.35) | | |

**Table IV The 6 miRNAs showed statistically significant down-regulation in the data of the 4 miRNA**

| miRNA | logFC | AveExpr | t | P.Value | adj.P.Val | B |
|---|---|---|---|---|---|---|
| hsa-miR-362-5p | -4.858160113 | 4.895317 | -5.97124 | 3.24E-06 | 0.000187363 | 4.423762 |
| hsa-miR-200c | -4.412839807 | 8.445282 | -5.35529 | 1.54E-05 | 0.000605192 | 2.882116 |
| hsa-miR-532-3p | -1.648789887 | 5.828535 | -4.73961 | 7.50E-05 | 0.001963873 | 1.324294 |
| hsa-miR-141 | -5.021573427 | 4.329796 | -4.33288 | 0.000214 | 0.004528746 | 0.296988 |
| hsa-miR-124 | -1.138192276 | 8.378763 | -4.01397 | 0.000486 | 0.008218573 | -0.50079 |
| hsa-miR-363 | -2.011720884 | 5.79213 | -3.21347 | 0.003626 | 0.038352499 | -2.4343 |

# Figures

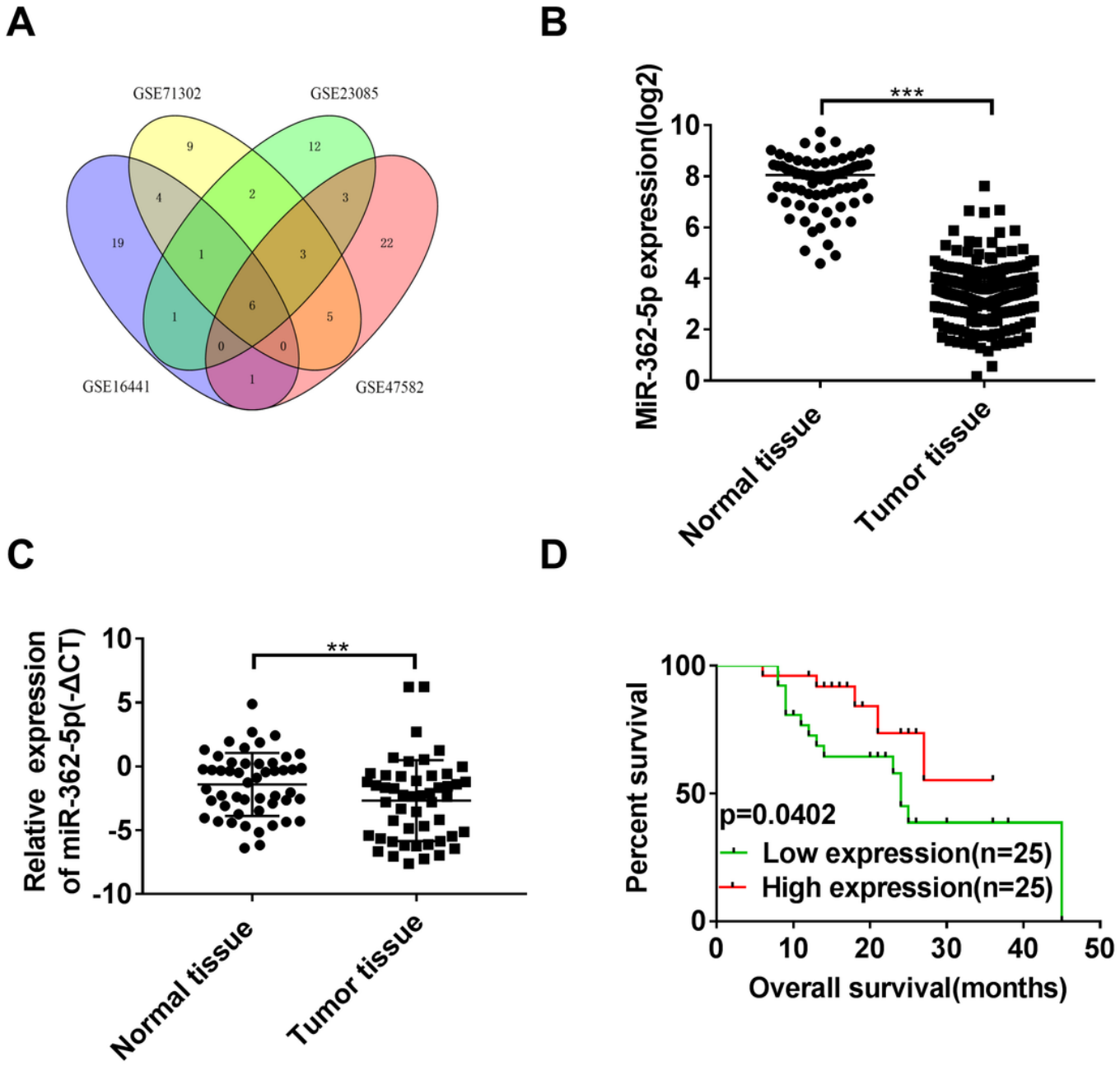


Figure 1

**MiR-362-5p is downregulated in clear cell renal cell carcinoma and correlated with patient survival and prognosis.**

**A:** Four groups of ccRCC and miRNAs matching downregulated miRNA expression profile microarray data in noncancerous renal tissues were intersected, and six miRNAs in the four miRNA expression profile microarrays were significantly downregulated. **B:** Relative expression of miR-362-5p in ccRCCs (n=249) and in noncancerous renal tissue samples (n=71) in a TCGA database. **C:** qRT–PCR was used to determine expression levels of miR-362-5p in 50 pairs of ccRCC and adjacent noncancerous tissue

samples, and the data were normalized to U6 expression levels. **D:** Kaplan–Meier survival curves of high and low expression miR-362-5p in ccRCC patients. “miR-362-5p low” (n= 25) represents the bottom samples, while “miR-362-5p high” (n = 25) represents the top samples (P=0.0402).

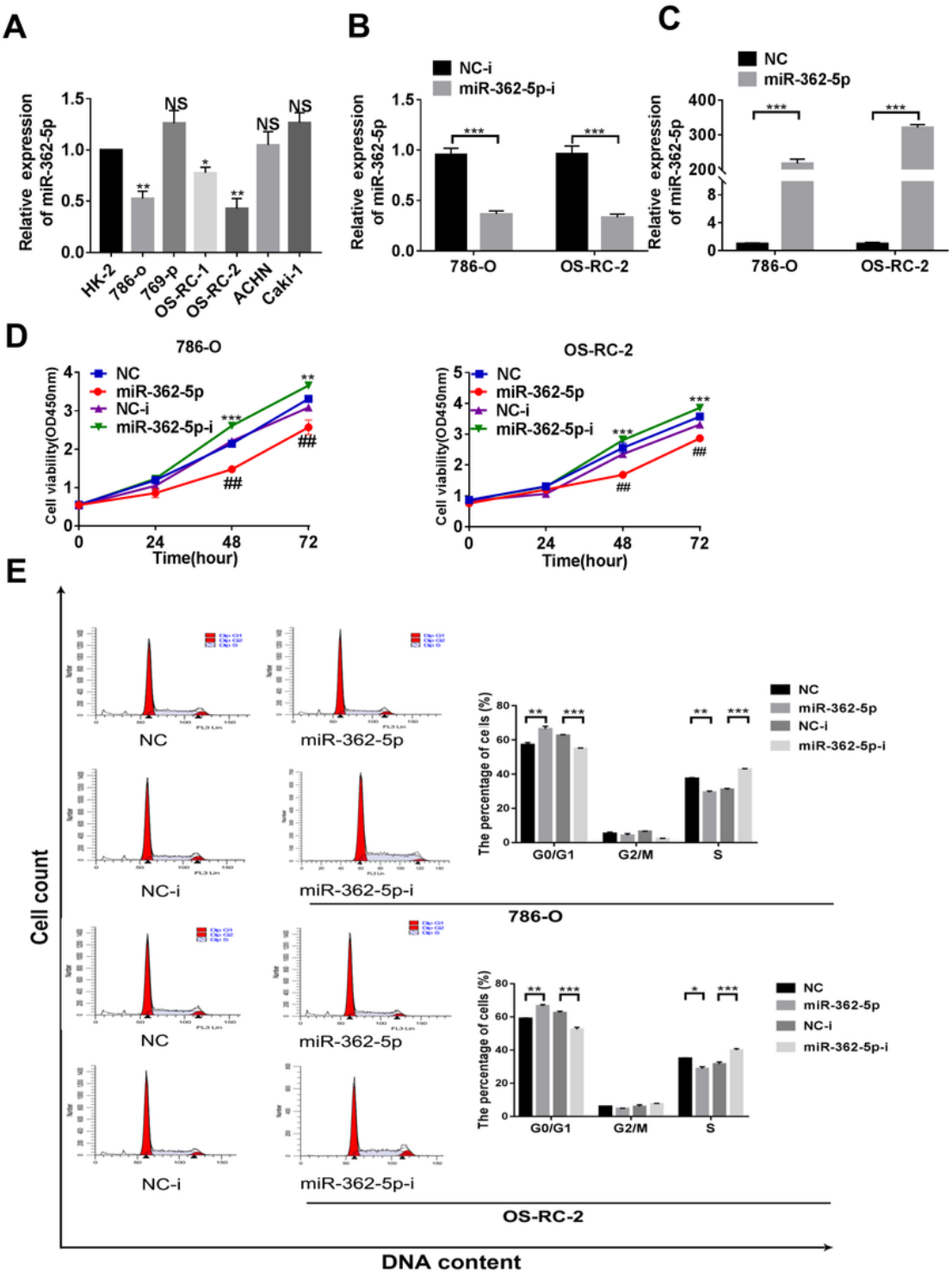


## Figure 2

**MiR-362-5p blocks cell cycle progression in clear cell renal carcinoma cells to inhibit cell proliferation.**

**A:** Expression levels of miR-362-5p in HK-2 cell lines and 6 ccRCC cell lines were detected by real-time PCR. Expression levels of miR-362-5p were decreased in some ccRCC cell lines. **B:** Transfecting a miR-362-5p inhibitor into 786-O and OS-RC-2 cells decreased the expression of miR-362-5p. Results were detected by qRT-PCR. **C:** Transfection of miR-362-5p mimic in 786-O and OS-RC-2 cells with real-time PCR analysis of miR-362-5p. **D:** After transfection with miR-362-5p mimic or miR-362-5p inhibitor, we used CCK-8 analysis to determine the effect of miR-362-5p on cell proliferation. **E:** Forty-eight hours after transfection of 786-O cells and OS-RC-2 cells, the cells were transfected with miR-362-5p or antagomiRNA, and cell cycle analysis was performed using flow cytometry. Representative histograms of cell cycle distribution and data analysis are shown. At least three independent experiments were performed to obtain the data. Data are shown as the mean ±SEM. *P 0.05; **P 0.01; ***P 0.001; NS, not significant.

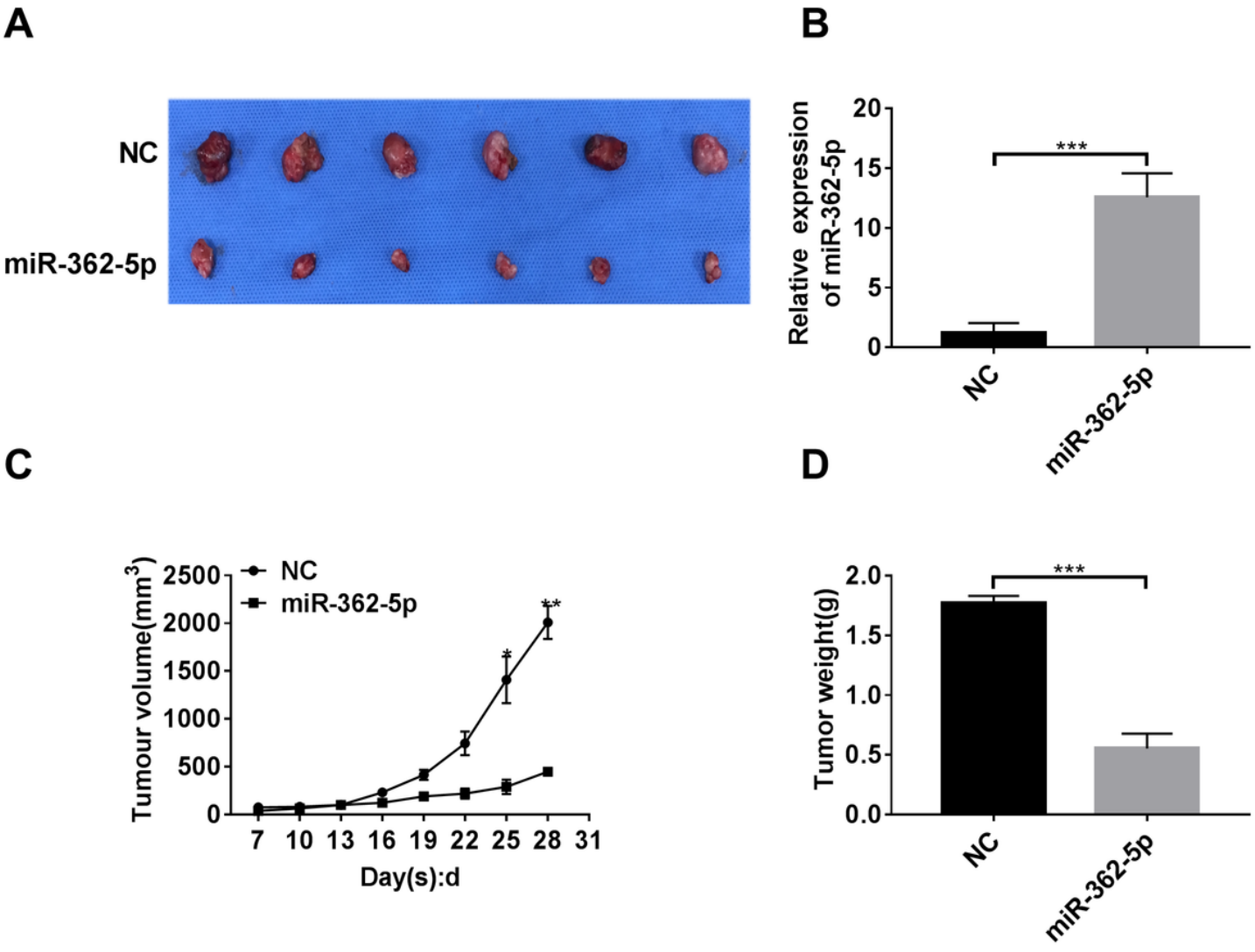


Figure 3

**MiR-362-5p restrains both cell proliferation and OS-RC-2 cell-derived tumor xenografts (n=6 mice).**

**A:** Using Lipofectamine 2000 (Invitrogen), OS-RC-2 cells were transfected with lentiviral vector LV10-NC or LV10-miR-362-5p, and $1*10^7$ stably transfected OS-RC-2 cells (100 mL PBS) were subcutaneously injected into the backs of BALB/c nude mice to form xenograft tumors. Twenty-eight days later, the mice were anesthetized and euthanized. Dissection of xenograft tumors in mice. **B:** Relative expression of miR-362-5p in the transplanted tumor tissues of mice injected with miR-362-5p or NC was analyzed by qRT–PCR. Expression is shown as a fold of NC. **C:** Tumor growth curves were determined by measuring the two vertical diameters every 3 days from days 7 to 28 by assessing tumor volume calculated using the following formula: $[(width)^2*length]/2$. **D:** The weight of xenograft tumors was measured on day 28.

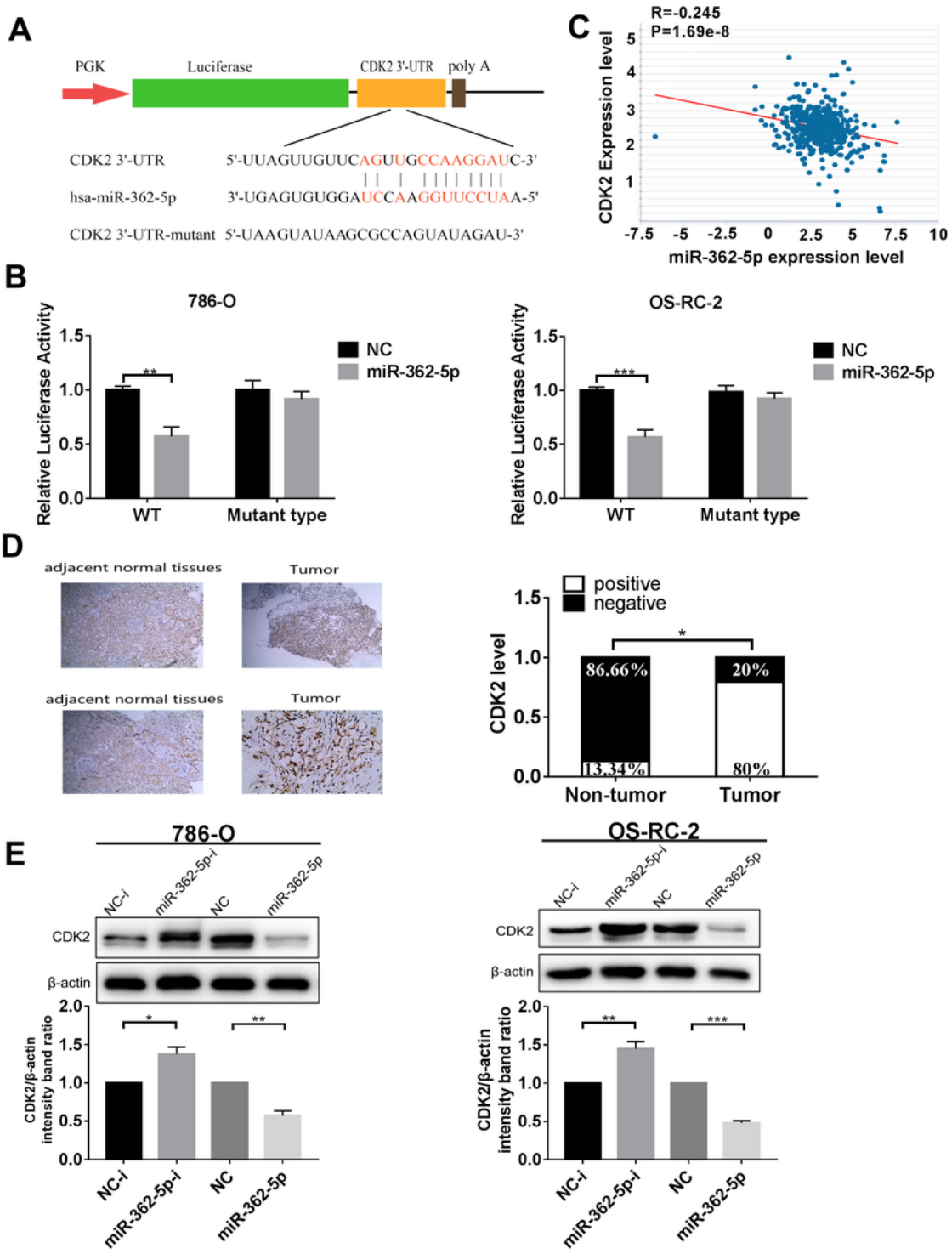


## Figure 4

**MiR-362-5p directly targets the CDK2 gene and downregulates CDK2 expression in ccRCC.**

**A:** Principal diagram of the predicted target binding site of miR-362-5p in the CDK2 3′-UTR. **B:** Detection of the luciferase activity of wild-type CDK2 3'-UTR (WT) and mutant CDK2 3'-UTR (Mut) in 786-O cells and OS-RC-2 cells. Two types of CDK2 were cotransfected with miR-362-5p mimics or miRNA negative control

(NC). **C:** Correlation between miR-362-5p and CDK2 expression in ccRCCs (TCGA, n = 249). **D:** Representative images of immunohistochemical staining of CDK2 (n = 15) and paired paracancerous (n = 15) images in human ccRCC tissues(left).Immunohistochemical results of 15 normal and 15 tumor tissues were statistically analyzed and plotted（right）.**E:** After transfection with miR-362-5p mimic, miR-362-5p inhibitor or negative control, we used western blot to detect the expression of CDK2 in ccRCC cells (top) using β-actin as a load control. The CDK2 bands were normalized to β-actin using ImageJ software (bottom).

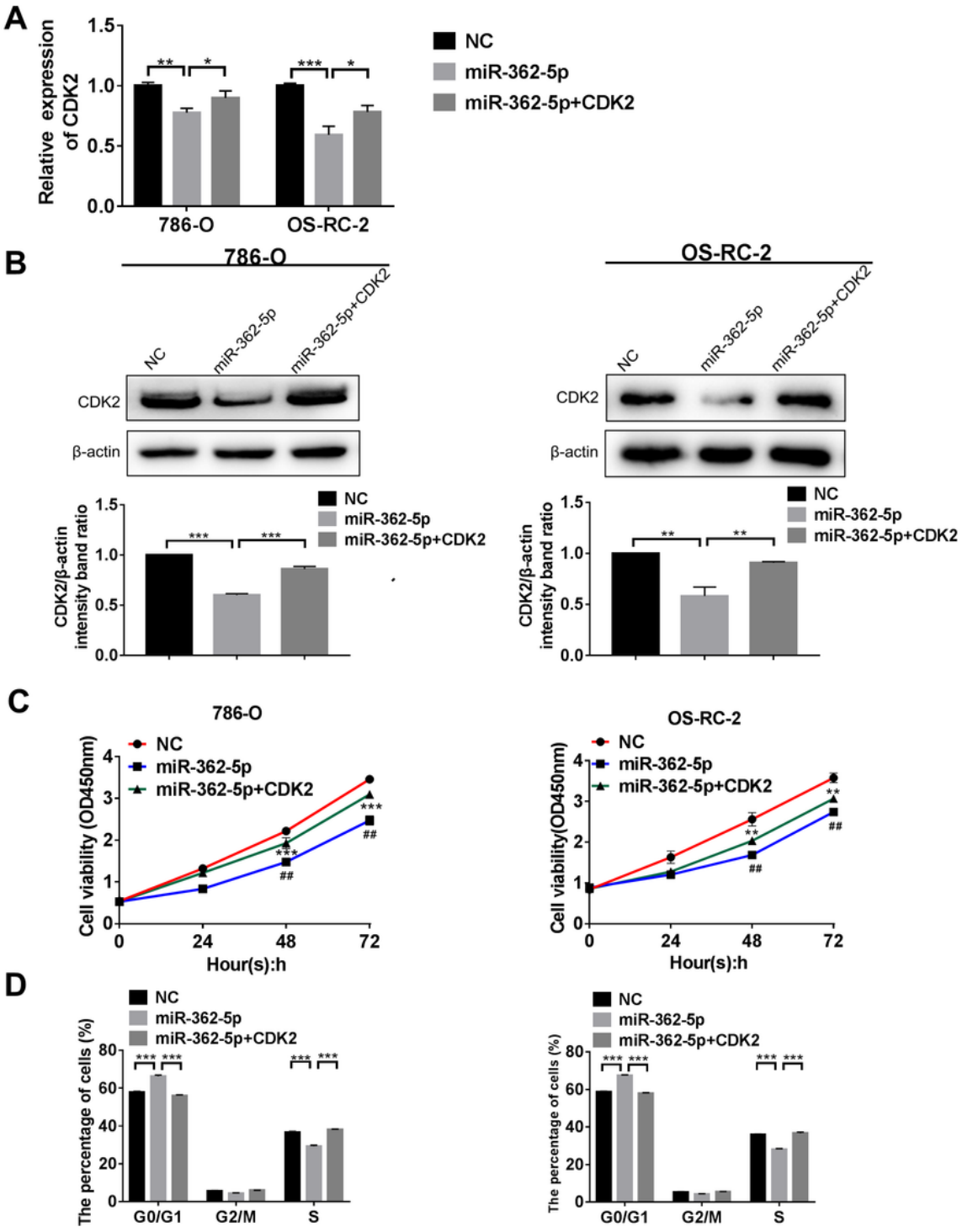

**Figure 5**

**CDK2 is involved in miR-362-5p-induced ccRCC cell growth inhibition.**

**A**: Negative control (NC), miR-362-5p mimic and miR-362-5p mimic+CDK2 were transfected into 786-O cells and OS-RC-2 cells, and then qRT–PCR was used to assess CDK2 expression levels. **B:** Western blot analysis of CDK2-transfected NC, miR-362-5p mimic and miR-362-5p mimic+CDK2 cells. β-actin was used as a negative control. **C:** Overexpression of CDK2 restored the inhibitory effect of overexpression of miR-362-5p on the growth rate of renal cell carcinoma cells. **D:** CDK2 overexpression reversed miR-362-5p-induced cell cycle arrest in 786-O and OS-RC-2 cell lines. *P 0.05; **P 0.01; ***P 0.001.

# Supplementary Files

This is a list of supplementary files associated with this preprint. Click to download.

- WBData.pdf